energies

MDPI

Article

Development of Greener D-Metal Inorganic Crosslinkers for Polymeric Gels Used in Water Control in Oil and Gas Applications

Hassan I. Nimir [1], Ahmed Hamza [2] and Ibnelwaleed A. Hussein [2,*]

[1] Department of Chemistry and Earth Sciences, College of Arts and Sciences, Qatar University, Doha P.O. Box 2713, Qatar; hnimir@qu.edu.qa

[2] Gas Processing Center, College of Engineering, Qatar University, Doha P.O. Box 2713, Qatar; Ahmed.Hamza@qu.edu.qa

* Correspondence: ihussein@qu.edu.qa

Received: 13 July 2020; Accepted: 11 August 2020; Published: 18 August 2020

Abstract: Crosslinkable polymers, such as polyacrylamide (PAM), are widely applied for water control in oil and gas reservoirs. Organic and inorganic crosslinkers are used to formulate a gel with PaM. Although chromium has a high level of toxicity, it has been implemented as an effective crosslinker combined with carboxylates because of the controllability of crosslinking time at low temperatures. The objective of this work was to develop greener d-metal inorganic crosslinkers based on cobalt, copper, and nickel to replace chromium for application at reservoir conditions. The obtained results showed that the gelation chemistry of the developed systems depends on the metal charge density. The gelation of PaM with d-metals depends on pH and temperature for low- and high-charge density, respectively. Cobalt (II) acetate (CoAc) was effective at high temperatures (130–150 °C) and forms (4% CoAc + 9%PAM) stable, and strong gels at a pH > 7 with a storage modulus exceeding 4300 Pa. However, Nickel Acetate and Cupper Acetate formed stable weak gels at low temperatures (50–70 °C) and a pH > 6 and gel decomposition was observed upon increasing the temperature. The developed formulations were compatible with low-salinity water (1000 ppm NaCl).

Keywords: cobalt (II) acetate; copper (II) acetate; nickle (II) acetate; polyacrylamide; inorganic crosslinking; polymeric gel

1. Introduction

The productivity of oil and gas wells is highly affected by the coproduction of water from water zones as well as the heterogeneity of the formations [1]. Sandstone reservoirs are associated with high permeability zones, whereas carbonates are naturally fractured. Crosslinked polymers have shown high efficiency in solving theses conformance control problems compared to conventional treatments such as mechanical sealing using Packers or cement squeezing [2–5]. Polyacrylamide (PAM) crosslinked by organic or inorganic crosslinkers is the most commonly applied type of polymer because of the ability to withstanding reservoir salinity and high-temperature conditions as well as its relatively low cost for field applications [2,6–10].

Inorganic crosslinkers are preferred for the low-temperature range because of their fast gelation at high temperatures (<2 h at temperature > 90 °C) compared to organic crosslinkers such as polyethyleneimine (PEI), which results in stable gel after crosslinking with PaM at high temperatures (>90 °C) [11]. Aluminum (III), chromium (III), zirconium (IV), and titanium (IV) have been used to crosslink polyacrylamides and polysaccharides [12,13].

The crosslinking between PaM and inorganic metals is established through ionic bonds [14–16]. The inorganic crosslinkers form a 3D gel structure with PaM through the formation of coordination

compounds [17,18]. Many theories, such as the ligand field theory (LFT), crystal field theory (CFT), valance bond theory (VBT), and molecular orbital theory (MOT), have been used to describe the bonding and interaction between metals and electron Pair donor known as ligands, which leads to the formation of coordination compound.

The stability of a complex compound (coordination compound) is a result of a release of energy accompanying the electrostatic or columbic interaction of the ligand electrons with the metal ion. The crystal field splitting energy (CFSE) quantifies the stability of the noncomplexed free metal ion in comparison to complex compounds in which metal-ligand bonds are formed in different geometries. Under the CFT, the degree and type of field (octahedral, tetrahedral, or square planar), charge, and size of metal ion affects magnitude of crystal field splitting energy, or the CFSE of d-orbitals. The magnitude of the field for a given metal ion and set of octahedral ligands is about twice as large as that of tetrahedral complexes. Square planar field splitting energies approximate those of octahedral fields [19–21]. Therefore, if the metal ions adopt octahedral or square planar geometry, then the charge density and the type of ligand dictate the strength of the coordination bond and, consequently, the gel strength.

Metal-carboxylate interactions depend on the nature of associations and the identity of the cation used. Group II metals reveal a mainly electrostatic interaction, while d-block metals can complex with carboxylate ligands resulting in more stable, pseudo-covalent bonds with reversible character [19]. The strength of complexation is further explained electronically by the ligand field stabilization energy, LFSE, of d-metal complexes. The stabilities of complexes formed by various metal follow some regular trends, which involve size and charge effects. One of the earliest correlations was the Irving-Williams series of stability. For divalent metal ions, the stability of period 4 metal complexes follows the trend of Ca < Mn < Fe < Co < Ni < Cu < Zn. Based on the geometry adopted by Zn (II), the order of Zn (II) and Ni (II) may change and is highly ligand-dependent [22]. This order arises in Part from a decline in size of metal ion across the series and in Part from ligand field effects [20].

For organic crosslinkers, such as PEI, the main disadvantage is the high crosslinking temperature (>90 °C), while the disadvantages of inorganic crosslinkers, such as chromium acetate, are toxicity and fast gelation [23,24]. Considering the shortcoming of Cr and Al, as well as the cost of using expensive metal such as Ti and Zr, metal crosslinking formulations that are stable around neutral pH conditions and form slow gel with PaM are needed. Development of inorganic crosslinkers for PaM gelation provides the oil and gas industry with an alternative for PEI. In this research, crosslinking of PaM using transition metal ion such as Co (II), Cu (II), and Ni (II), which are of lower toxicity in comparison with Cr, was investigated. Moreover, insights on gel chemistry were provided and the influence of temperature, pH and salinity on gelation and gel properties was investigated. Furthermore, the compatibility of the developed system with saline water and nanosilica was addressed.

2. Gelation Mechanism of Inorganic Crosslinkers

The proposed mechanism of crosslinking of PaM and its derivatives using Cu (II), Co (II), or Ni (II) simple acetates was functioned through complexation. The metal ion coordinated with the polymer through the nitrogen of the amine and other ligation to complete the preferred stable geometry. The stability of the complex could be explained by quantizing the CFSE of the d-metal complex. CFSE was affected by the charge density of the metal ion, geometry of the complex, and the electrostatic field of the ligands, including the solvent water, polymer (amide), and acetate.

At high pH or temperature, PaM undergoes hydrolysis when the labile amide moiety R-$CONH_2$ hydrolyzes leading to the evolution of ammonia and a carboxyl group R-COO^-, as shown in Figure 1 [25,26].

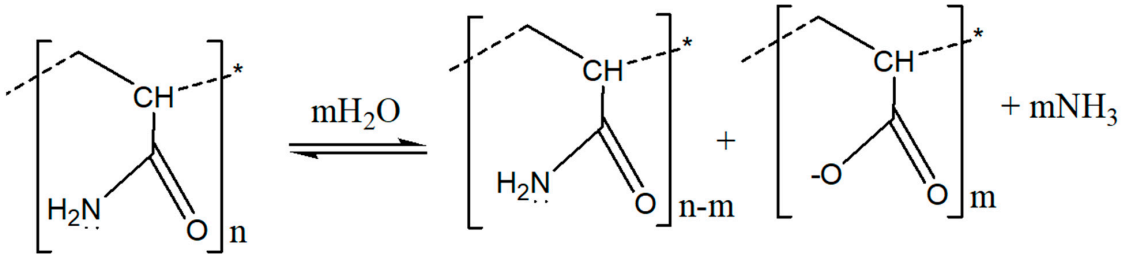

Figure 1. Polyacrylamide (PAM) hydrolysis in water to form hydrolyzed HPAM and ammonia.

The metal carboxylate dissolves in water to form aqua complexes with d-metal. These aqua complexes, exemplified by the octahedral complex, $[M(H_2O)_6]^{n+}$, undergo substitution reactions in solution with the available ligands, such as amide, carboxylates moieties in the HPAM, and chloride ions in saline conditions. Ligand substitution reactions are among the most fundamental reactions a complex can undergo. This class of reaction comprises complex formation, in which the leaving group, the displaced ligand, X, is a solvent and the entering group the displacing ligand, Y, is some other ligand as in Equation (1):

$$[M(H_2O)_6]_{n+} + Y \leftrightarrow [M(Y)(H_2O)_5]_{n+} + H_2O \quad (1)$$

The rate of substitution reaction spans a very wide range and correlates with the structures of the complexes. In general, complexes of metal ions that have no extra factors to obtain additional stability, such as strong chelate effect and/or LFSE effect, are among the most labile with respect to substitution reactions. Complexes that show fast substitution are known as labile, while those associated with slow rates are known as inert or nonlabile. Any additional stability of the complex results in an increase in activation energy for a ligand replacement reaction and hence reduces the lability of the complex. Generally, very small ions are often less labile because they have greater M-L bond strengths, which makes it very difficult for incoming ligands to approach the metal atom closely [22,27].

Across the 3d series, complexes of d-metal M (II) ions are generally moderately labile, with distorted Cu (II) complexes among the most labile. Complexes of d-metal, M (III) ions are distinctly less labile than d-metal, M (II) ions. The d-Metal complexes with d^3 and low-spin d^6 configurations (for example, Fe (II), Cr (III), and Co (III)) are mostly nonlabile. Figure 2 reveals the crosslinking mechanism through complexation explained by formation of octahedral complex.

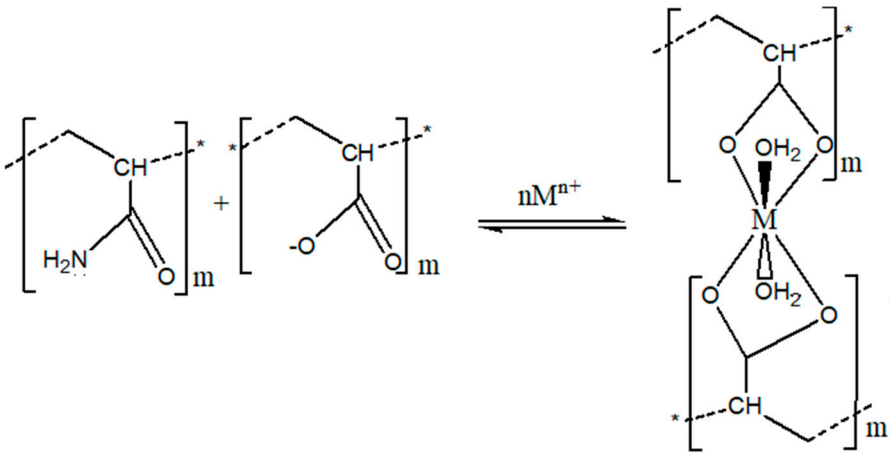

Figure 2. Proposed mechanism of PaM crosslinking through metal complexes formation.

The nature of associations depends on the characteristics of the cation used. Group II metals show a mainly electrostatic interaction, while d-block metals can complex with carboxylate ligands leading to more stable, pseudo-covalent bonds with reversible character. The bond stability of complexes formed

follows the Irving Williams series, which basically scales with decreasing cation size [22]. The decrease in cation size indicates an increase in cation charge density or charges over radius ratio. However, the trend is further explained by the effect of electronic configuration through ligand field stabilization energies (LFSE) up to d^8 metals. For the ions used in this study, this trend follows Co (II) < Ni (II) < Cu (II). Copper (II) has lower LFSE energies than Ni (II), which can be attributed to the geometry of the complex. Cu (II) complexes reveal tetragonal distortion of the octahedral geometry because of the Jahn-Teller effect [12].

Table 1 illustrates the charge/radius ratio (charge density) of different metals. Cr (III) and Al (III) have a higher charge/radius ratio (charge density), which gives a clear explanation of the behavior of their stronger gelation properties compared to 3d metal M (II) cation in this study. The gelation properties for the M (II) [M = Co, Ni, Cu] decreased from cobalt to copper, which correlates very well with the drop in charge density. The effect of metal charge to size ratio has been addressed for hydrogels in previous studies [28].

Table 1. Charge to radius ratio of different metals.

Metal Ion	Electron Configuration	Ionic Radius * (O_h Geometry) in pm	Charge/Radius Ratio (pm^{-1})
Al (III)	[Ne]	39.00 (4), 53.00(6)	3/53.00 = 0.0566
Cr (III)	$[Ar]3d^3$	62.00 (6)	3/62.00 = 0.0484
Co (II)	$[Ar]3d^7$	65.00 (6)	2/65.00 = 0.0308
Ni (II)	$[Ar]3d^8$	55.00 (4), 69.00 (6)	2/69.00 = 0.0289
Cu (II)	$[Ar]3d^9$	73.00 (6)	2/73.00 = 0.0274

* ionic radius in pm & coordination number in Parentheses. Ionic radius data from Shannon [29].

All these complexes for M (III) or M (II) are affected by pH because at lower pH, the proton H^+ competes with the metal ion in the solution and facilitates hydrolysis and complex instability. Whereas, in basic solution, the hydroxyl group acts as ligand as well, and eventually lead to hydrolysis of HPAM-Metal complex, as confirmed in case of Ti due to ligand competition and formation of polynuclear Ti oxo/hydroxo-complexes [13].

3. Experimental Work

3.1. Materials and Preparation Steps

Low molecular weight (MW) (700,000 Da) polyacrylamide (PAM) polymer was received from SNF Fogler, France. Copper (II) acetate monohydrate (CuAc) ($Cu(CH_3\text{-}OO)_2$). H_2O (MW 199.65) and anhydrous Cobalt (II) acetate (CoAc) $Co(CH_3COO)_2$ (MW 177.02) were purchased from Glentham Company, UK. Nickel (II) acetate (tetrahydrate) (NiAc) $Ni(CH_3.COO)_2$, and $4H_2O$ (MW 248.84) was acquired from the Biochem Chemopharma Company, France. Nanosilica (50 nm) was acquired from NYACOL Nano Technologies, Inc., Canada. High salinity seawater was prepared using salts with total dissolved solids (TDS) 65.3 gm/Liter. The initial pH was adjusted using droplets of concentrated potassium hydroxide (KOH) solutions (20 wt.%).

All solutions were prepared using deionized water, except high salinity experiments, in which seawater was mixed with the polymer. The preparation steps were as follows: The water phase was added to PaM first, followed by additives such as salts and nanosilica. Then, the crosslinking metal (Co (II), Cu (II), or Ni (II)) acetate was added as drops, and pH was adjusted using KOH, if necessary, in the final step. The formulations containing nanosilica were subjected to sonication for 10 min to assure good distribution of nanosilica Particles in the solution.

3.2. Characterization

Thermogravimetric analysis (TGA) was conducted for Cobalt (II) acetate to investigate the effect of temperature on the sample up to 200°C at a scanning rate of 5 °C/min with a waiting period at 105 °C and 130 °C for 15 min at each point. Ultraviolet-visible spectroscopy (UV-Vis) and Fourier-transform infrared spectroscopy (FTIR) were done to evaluate the bonds of the PaM and polymeric gels formulated by cobalt acetate.

3.3. Rheology Measurements

The effect of temperature was investigated by immersing the polymeric solutions within test GL-80 tubes in an oil bath for one day at room temperature, 70 °C and 130 °C, to simulate the conditions of oil and gas reservoirs. The Sydansk [30] gel coding system was applied to visually evaluate each formed gel. The rheological properties such as storage modulus and loss modulus, were studied using an Anton Par rheometer (MCR 302) using Parallel plate geometry with a 2-mm gap and fixed strain 1% at room temperature (25 °C). Additionally, the effect of initial pH on the rheological characteristics was investigated at different temperatures of 25 °C, 70 °C, and 130 °C.

4. Results and Discussion

4.1. Rheological Behavior and Viscoelastic Properties of the Inorganic Gels

Cobalt (II), copper (II), and nickel (II) acetates were used to crosslink 9% PaM. Each metal ion showed different behavior during the crosslinking. However, all metal ions were influenced by pH. Cobalt crosslinked with PaM at a high temperature (130 °C) and a pH of 7.3, while copper and nickel were able to crosslink at room temperature and a pH of higher than 6. Nevertheless, nickel showed better stability range (up to 70 °C) in comparison with copper (up to 50 °C). The minimum amount used to crosslink 9 wt.% PaM was about 10,000 ppm of Co (II). However, using a similar concentration for Cu (II) and Ni (II) did not crosslink PaM at the same conditions (130°C). Gel formation as a result of the crosslinking of PaM and cobalt acetate was achieved in the range of 3–4.5 wt.% CoAc. Depending on the Co (II) concentration in the formulation, the formed gels showed different gel strength, as characterized by Sydansk codes [30]. Table 2 reveals the Sydansk codes after crosslinking PaM with CoAc.

Table 2. Crosslinking of 9% PaM with CoAc at a pH of 7.3.

Cobalt (II) Concentration, ppm	Sydansk Code	Observation
330	A	No gel was detected at low or high temperatures (25–150 °C)
3300	A	No gel was detected at low or high temperatures (25–130 °C)
10,000	E-D	The gel started to move when the temperature decreased from 130 °C to 25 °C.
12,000	F-E	Part of the gel started to move when the temperature decreased from 130 °C to 25 °C.
13,300	F-E	Part of the gel started to move when the temperature decreased from 130 °C to 25 °C.
16,700	A	No gel was detected at low or high temperatures (25–130 °C)

CoAc formed a gel at high temperature (130–150 °C) only, while no gel was detected at lower temperatures. The minimum concentration of CoAc that provided a gel was 10,000 ppm (3wt.) (Sydansk code "E-D"), which showed a barely flowing gel (Figure 3). Increasing the concentration up to 13,300 ppm (4.5 wt.%) enhanced the gel strength. After that, no gel was detected. This could tentatively

be due to the thermal instability of the HPAM metal complex and competition from other Oxo/or hydroxide ligand substitution equilibria that decrease the strength of the desired PaM-Co complex.

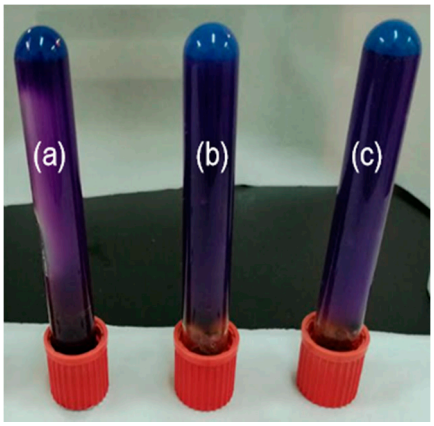

Figure 3. Crosslinking 9% PaM with various concentrations of Co (II): (**a**) 10,000 ppm, (**b**) 12,000 ppm, and (**c**) 13,300 ppm at 130 °C.

Increasing the concentration of CoAc from 10,000 ppm to 13,300 ppm (3 to 4.5 wt.%) increased the storage modulus of the gels from 24 Pa (weak gel) to 4300 Pa (strong gel) at a pH of 7.3 (Figure 4). The obtained storage modulus using 4.5 wt.% cobalt (II) acetate with 9 wt.% PaM was comparable with the currently used organic and inorganic crosslinkers such as PEI and chromium acetate. The storage modulus of 9 wt.% PaM/1 wt.% PEI was around 1700 Pa at 130 °C [31]. Chromium (III) acetate at lower concentration (50–500 ppm) compared to cobalt (II) can crosslink PaM at temperature > 90°C. In another study by our group, 0.5 wt.% chromium acetate was used to crosslink 9 wt.% polyacrylamide-co-tert-butyl acrylate (PAtBA) at 90°C, providing a gel with a storage modulus of 1280 Pa. PaM/chromium (III) showed a high crosslinking rate at high temperatures (90–135 °C) [32,33]. Therefore, cobalt can be a green crosslinker alternative to PEI and chromium (III) at high temperature conditions, especially for gas reservoirs, where the temperature is in the range between 130–150 °C.

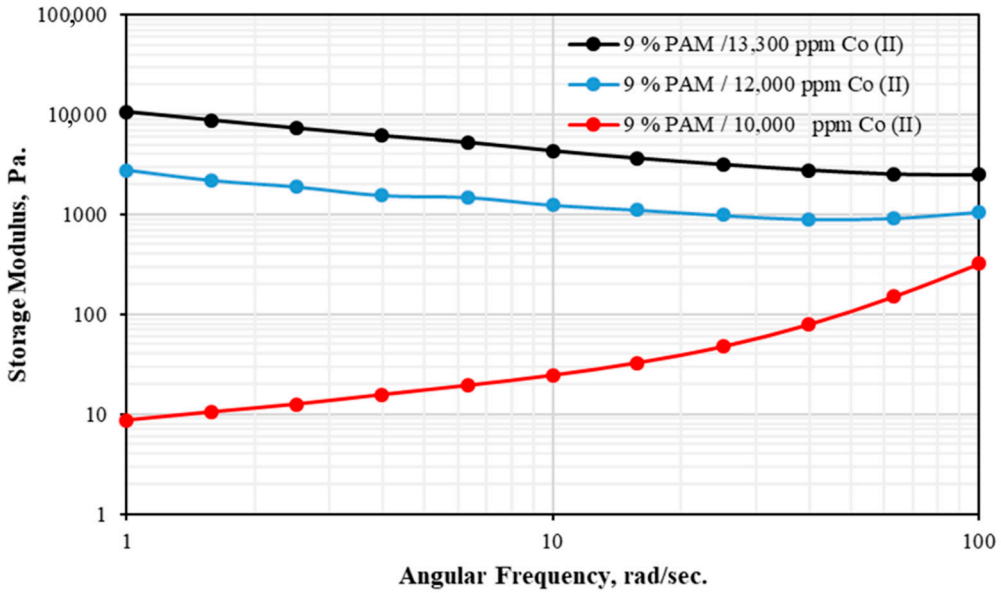

Figure 4. Effect of Co (II) concentration on mature gel storage modulus (25 °C, pH = 7.25).

In contrast, CuAc based gels were formed at a minimum pH of 6. Figure 5 shows the flow behavior of the 11,145 ppm Cu (II) (3.5 wt.% CuAc)/9% PaM gel formed at room temperature at pH of 10.4.

The decreasing trend of viscosity as the shear rate increased depicts that the flow behavior of this type of gels follows non-Newtonian shear-thinning behavior with yield stress at rest. The developed weak gels by crosslinking of PaM/CuAc could be useful for other applications such as enhanced oil recovery.

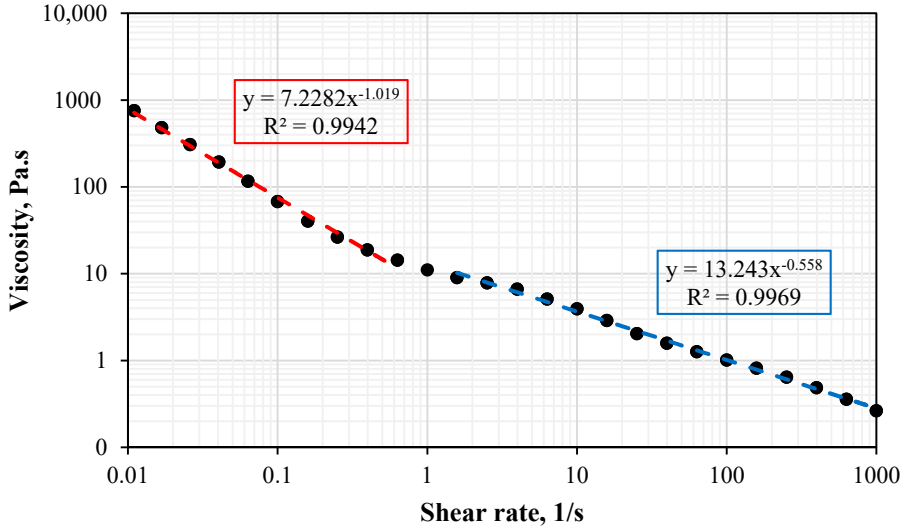

Figure 5. Flow behavior of CuAc gels at a pH of 10.4 and 25 °C.

All the measurements were done at least twice to confirm the repeatability of the obtained results. On average, the uncertainty in the rheological measurements is 5%. Proper mixing of the polymer/crosslinkers and adjusting the pH are vital for developing homogenous gels and obtaining consistent results.

4.2. Investigation of the Effect of Temperature on Gel Strength

CoAc with Co (II) concentration in the range of 10,000 ppm to 13,300 ppm (3–4.5 wt.% CoAc) formed gels with 9% PaM at 130 °C to 150 °C, whereas both CuAc and NiAc failed to compose a gel at these conditions. Black precipitation of copper oxide was observed when 9% PaM/11,145 ppm Cu (II) heated up to 130 °C (Figure 6). For NiAc, the formed gel was able to withstand temperature up to 70 °C, whereas the CuAc gel decomposed at that level at a similar pH (>6).

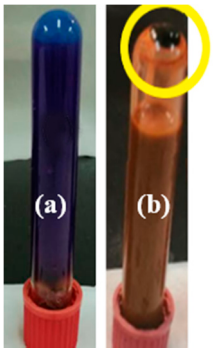

Figure 6. Physical appearance of gel: (**a**) Gels formed after crosslinking 9% PaM/12,000 ppm Co (II) at 130 °C and (**b**) copper oxide precipitation after heating 9% PaM/11,145 ppm Cu (II) at 130 °C.

The TGA analysis of the CoAc showed insignificant weight loss (Figure 7) at the temperature range of 130–150 °C, which indicates no transition of the CoAc structure.

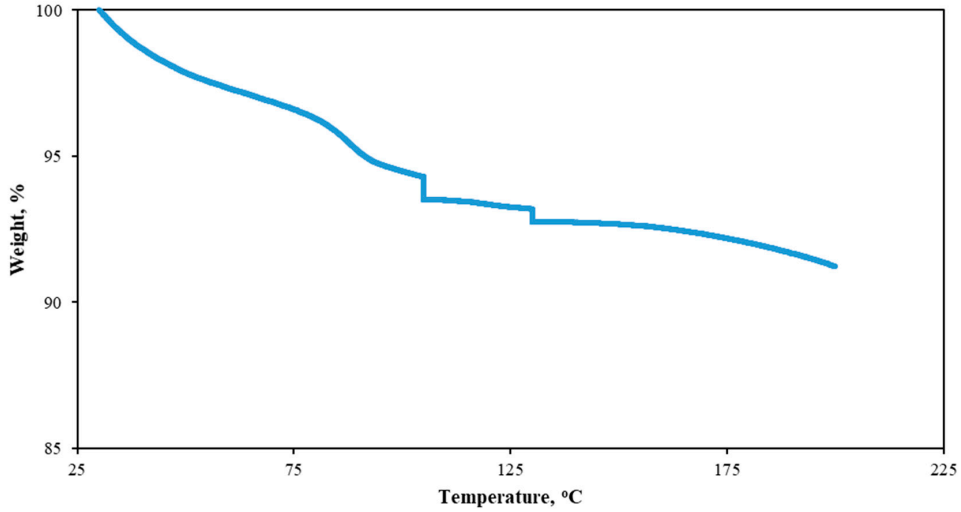

Figure 7. Thermogravimetric analysis (TGA) of CoAc.

Figure 8 shows the UV-visible analysis of 9 wt.% PaM and 9 wt.% PaM/12,000 ppm Co (II). An increase in the absorbance percentage along the wavelength from 320 nm to 900 nm after adding CoAc.

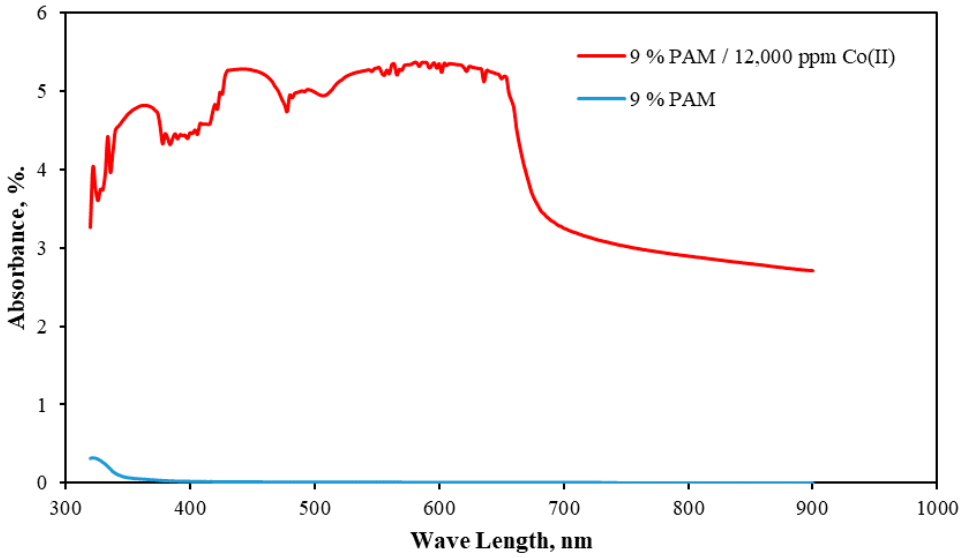

Figure 8. Ultraviolet-visible spectroscopy (UV-Vis) analysis of 9 wt.% PaM and 9 wt.% PaM/12,000 ppm Co (II) mature gel.

FTIR analysis (Figure 9) of 9 wt.% PaM and 9 wt.% PaM with 12,000 ppm Co (II) gel sample revealed the main bonds associated with the peaks and the change in wavenumber after the crosslinking. Table 3 illustrates the interpretation of the peaks assigned for the peaks of 9 wt.% PaM and mature gel composed of crosslinking 9 wt.% PaM with 12,000 ppm Co (II). The peaks were assigned as follows: 3317–3262 cm^{-1} for secondary amide N-H stretching, 2871 cm^{-1} for C-H bond stretching, 1550–1636 cm^{-1} for primary amide C=O stretching, and 475–491 cm^{-1} C-C and 413–460 O-C-N bending, respectively [34–36]. The significant change was observed in the carbonyl group bond, which confirms the crosslinking mechanism.

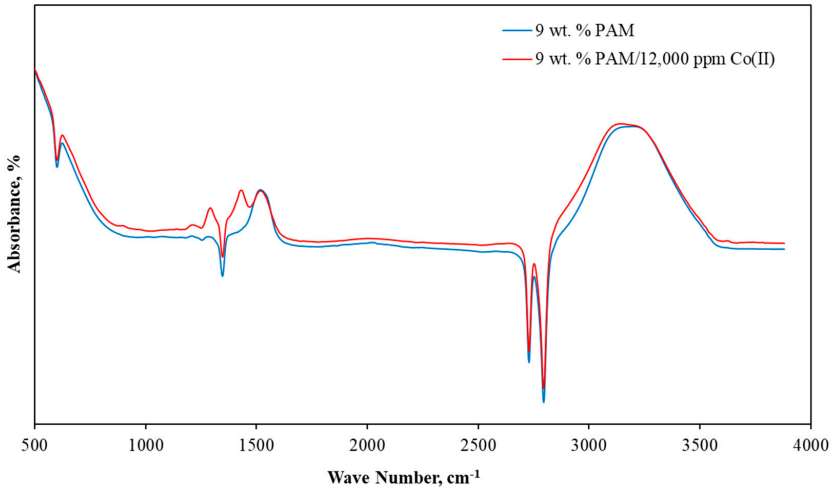

Figure 9. Fourier-transform infrared spectroscopy (FTIR) of 9 wt.% PaM and 9 wt.% PaM/12,000 ppm Co (II) mature gel.

Table 3. Functional group analysis using FTIR.

Wave Number, cm^{-1}		Assigned Bond
9 wt.% PaM	Mature Gel 9 wt.% PaM/12,000 ppm Co (II)	
3317	3262	Secondary amide N-H stretching
2871	2871	C-H bond stretching
1636	1550	Primary amide C=O stretching
491	490	C-C
475	475	
460	460	O-C-N Bending
444	440	
430	428	
413	-	

4.3. Effect of PH

The working range of pH to initiate the gelation of the inorganic crosslinkers was above 6. Copper and nickel acetate composed gels with 9% PaM at pH > 6. At basic conditions, gels were observed even at room temperature, indicating the impact of pH on the crosslinking reaction for these two metals. Increasing the pH enhanced gel strength and stability. On the Sydansk gel coding system, the formed gels based on Cu (II) and Ni (II) acetate can be classified as class "E" and "F" at a pH of 8 and 11, respectively. However, the formed gels were not homogeneous and liquid phase could be observed in the samples. Table 4 and Figure 10 depict the influence of pH on the formed gels by CuAc at different concentrations.

Table 4. Effect of pH on the stability of the gel formed by 9 wt.% PaM/CuAC.

Concentration of Cu (II), ppm	pH	Sydansk Code	Observation
300–14,300	5.23	A	No gel was detected at low and high temperatures.
11,145	7	B-C	Increasing the initial pH of the solution improved the gel strength at room temperature up to class G.
11,145	11	E-G	

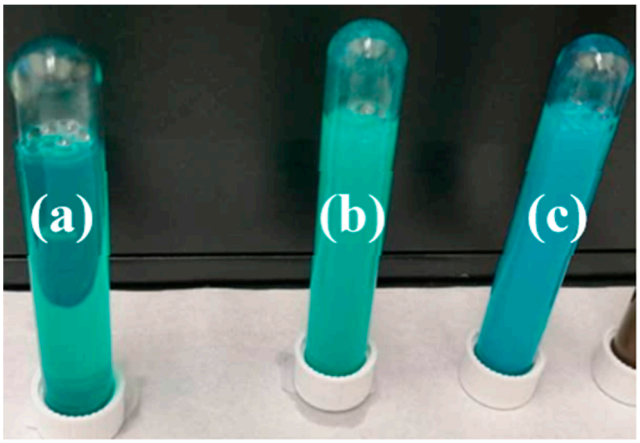

Figure 10. Gel formed by CuAc at room temperature at various pH values: (**a**) No gel at pH = 5.23 and weak gel at (**b**) pH = 7 and (**c**) pH = 11.

The effect of pH on the storage modulus after crosslinking 9% PaM with 3.5% CuAc at different pH values is shown in Figure 11. It can be clearly seen that there was an optimum for the pH, since at a low pH of 5.23, no gel was formed, while increasing the pH to 7 and 11 raised the storage modulus to 21 Pa and 179 Pa, respectively. In contrast to CuAc, NiAc showed a decreasing trend for the storage modulus with an increase in pH (Figure 12). However, the gels were not homogeneous and this can be seen visually in Figure 13. Therefore, at a neutral pH of 7, the formed Particles of the gels were stronger than the more homogeneous gels at a strong basic pH of 12. This heterogeneous behavior could be useful in other applications such as forming microgels. Both carboxylate ligands and the charged states of metallic cations are affected by pH. Complex formation and binding modes in these experiments are highly pH-dependent. Little complexation exists under basic conditions because of hydroxide formation, which diminishes the polyvalent state of a hydrated cation [37].

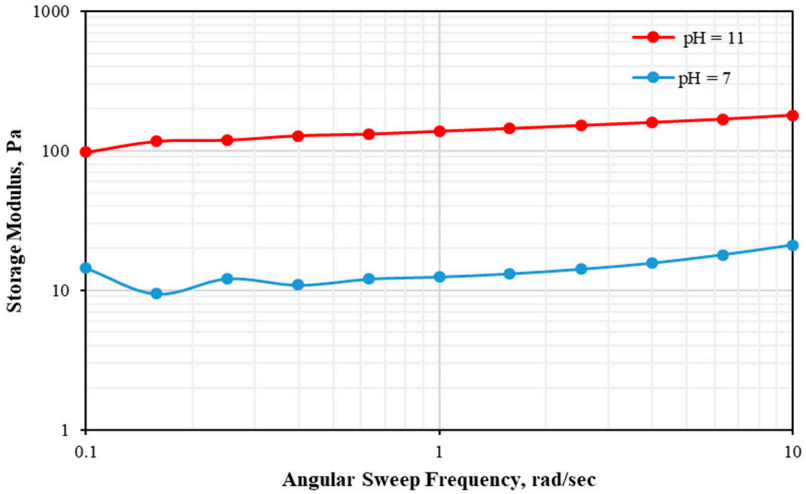

Figure 11. Effect of pH on the storage modulus of gels composed of 3.5% CuAc/9% PaM (25 °C).

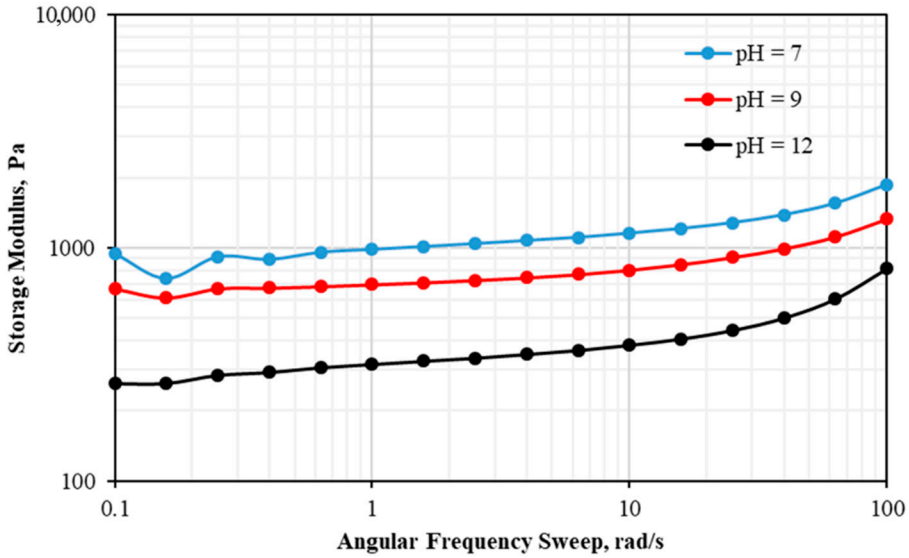

Figure 12. Effect of pH on the storage modulus of gels composed of 4% NiAc (9450 ppm Ni)/9% PaM (T = 25°C).

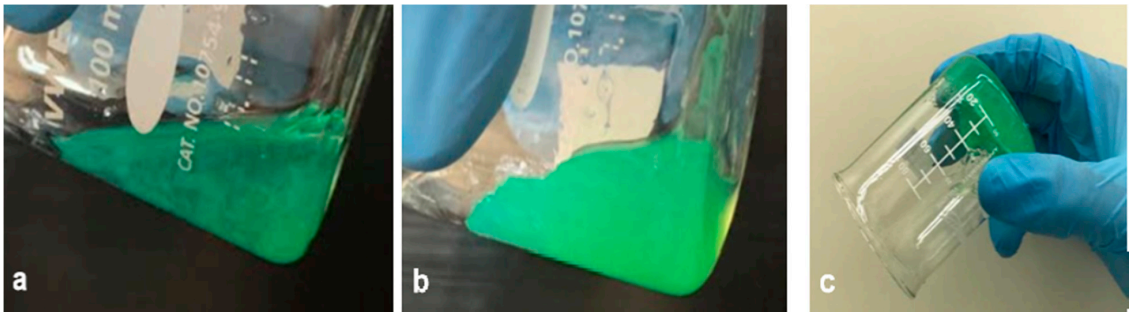

Figure 13. Effect of pH on the gel strength composed of 3.5% NiAc (8260 ppm Ni)/9% PaM, (**a**) pH = 6.3, (**b**) pH = 8, and (**c**) pH = 12.

4.4. Gel Compatibility with Additives

Generally, salts work as retarders to the gelation of the crosslinked gels [26,38]. Adding 0.1% NaCl decreased the storage modulus of the gel formed of 3.5% CoAc/9% PaM by 70% to about 360 Pa (Figure 14), whereas no gels were identified at higher salt concentrations and when seawater was used. For copper and nickel, no gels were detected when NaCl or seawater were used. Nanosilica is generally used to reinforce the crosslinked gel [9,39–41]. However, no gels were formed for all used types of d-metal crosslinkers when nanosilica (1000–20,000 ppm) to reinforce the inorganic gels. This can be explained by the competitive behavior between the silanol group in the nanosilica and the metals to form a bond with PAM.

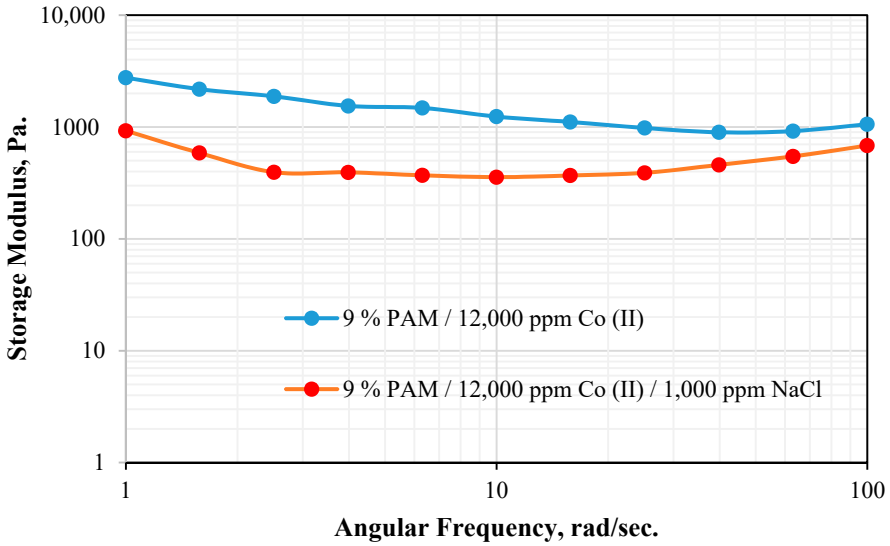

Figure 14. Effect of adding 1000 ppm NaCl on the storage modulus of the gel (T = 25 °C).

4.5. Environmental Impact of Inorganic Crosslinkers

The health and environmental impact of the chemical materials was generally evaluated using a lethal dose (LD_{50}). A LD_{50} can be explained as the amount of substance taken all at once that can cause the death of half of the tested group. Table 5 reveals the lethal dose of d-metals versus chromium and titanium. The average lethal dose of the transitional metals used in this study was higher than that of chromium, which is widely used in the oil industry. Therefore, this an indication that cobalt, nickel, and copper are safer than chromium, with less environmental impact on the environment than chromium.

Table 5. Lethal dose of inorganic crosslinkers.

Type	LD_{50} (mg/kg body)	Reference
Cr (VI)	250	[2]
Cr (III)	615	[2]
Co (II)	3672	[42,43]
Ni (II)	11,000	[44]
Cu (II)	1600	[45]
Ti (IV)	2775	[46]

5. Conclusions

In this study, inorganic crosslinked polymeric gels were formulated using cobalt (II), copper (II), and nickel (II) acetates at high (130°C) and low (up to 70°C) temperatures and at intermediate to high pH. The following conclusions can be made: The crosslinking of PaM with d-metals depends mainly on metal charge density.

Cobalt (II) acetate was able to crosslink with 9 wt.% PaM at 130°C, showing a strong gel with a storage modulus exceeding 4300 Pa when 13,300 ppm Co (II) (4.5 wt.% CoAc) was used.

Copper (II) acetate and nickel (II) acetate were affected by pH and gels formed at lower temperatures between 50 °C–70 °C. However, these gels decomposed at higher temperatures.

For nickel (II) acetate solutions, the gel strength decreased as the pH increased and vice versa for copper (II) acetate samples.

Copper (II) acetate gels exhibited shear thinning behavior.

The developed inorganic systems were not compatible with high salinity. A low concentration of NaCl (1000 ppm) hindered the crosslinking of PaM/cobalt (II) acetate, and no gels were detected at higher salinity levels.

When nanosilica was used to enhance the gel strength, competitive binding between silanol and metal toward PaM chains prevented the gelation process.

Author Contributions: Conceptualization, H.I.N., A.H. and I.A.H.; methodology, H.I.N., A.H. and I.A.H.; validation, H.I.N., A.H. and I.A.H.; data curation, A.H.; writing—original draft preparation, H.I.N. and A.H.; writing—review and editing, H.I.N., A.H. and I.A.H.; supervision, H.I.N. and I.A.H.; project administration, I.A.H.; funding acquisition, I.A.H. All authors have read and agreed to the published version of the manuscript.

Funding: This research was funded by of Qatar National Research Fund (a member of Qatar Foundation), grant number NPRP10-0125-170240.

Acknowledgments: The authors would like to acknowledge the support of Qatar National Research Fund (a member of Qatar Foundation) through grant # NPRP10-0125-170240. Special thanks with gratitude to SNF Company, France, for supplying the polymers used in this study. The findings achieved herein are solely the responsibility of the authors. Hassan Nimir wish to dedicate this Paper to the memory of his late PhD Supervisor and friend David A. Brown of the University College Dublin, Republic of Ireland.

Conflicts of Interest: The authors declare no conflict of interest.

References

1. Elsharafi, M.O.; Bai, B. Influence of strong preformed Particle gels on low permeable formations in mature reservoirs. *Pet. Sci.* **2016**, *13*, 77–90. [CrossRef]
2. Hamza, A.; Shamlooh, M.; Hussein, I.A.; Nasser, M.; Salehi, S. Polymeric formulations used for loss circulation materials and wellbore strengthening applications in oil and gas wells: A review. *J. Pet. Sci. Eng.* **2019**, *180*, 197–214. [CrossRef]
3. Bai, Y.; Xiong, C.; Wei, F.; Li, J.; Shu, Y.; Liu, D. Gelation study on a hydrophobically associating polymer/polyethylenimine gel system for water shut-off treatment. *Energy Fuels* **2015**, *29*, 447–458. [CrossRef]
4. Bai, Y.; Wei, F.; Xiong, C.; Li, J.; Jiang, R.; Xu, H.; Shu, Y. Effects of fracture and matrix on propagation behavior and water shut-off performance of a polymer gel. *Energy Fuels* **2015**, *29*, 5534–5543. [CrossRef]
5. Li, T.; Fang, J.; Jiao, B.; He, L.; Dai, C.; You, Q. Study on a novel gelled foam for conformance control in high temperature and high salinity reservoirs. *Energies* **2018**, *11*, 1364. [CrossRef]
6. Bkour, Q.; Faqir, N.; Shawabkeh, R.; Ul-Hamid, A.; Bart, H.J. Synthesis of a Ca/Na-aluminosilicate from kaolin and limestone and its use for adsorption of CO_2. *J. Environ. Chem. Eng.* **2016**, *4*, 973–983. [CrossRef]
7. El-Karsani, K.S.M.; Al-Muntasheri, G.A.; Sultan, A.S.; Hussein, I.A. Gelation of a water-shutoff gel at high pressure and high temperature: Rheological investigation. *SPE J.* **2015**, *20*, 1103–1112. [CrossRef]
8. Godwin Uranta, K.; Rezaei-Gomari, S.; Russell, P.; Hamad, F. Studying the effectiveness of Polyacrylamide (PAM) Application in hydrocarbon reservoirs at different operational conditions. *Energies* **2018**, *11*, 2201. [CrossRef]
9. Raghav Chaturvedi, K.; Kumar, R.; Trivedi, J.; Sheng, J.J.; Sharma, T. Stable silica nanofluids of an oilfield polymer for enhanced CO_2 absorption for oilfield applications. *Energy Fuels* **2018**, *32*, 12730–12741. [CrossRef]
10. Azad, M.S.; Dalsania, Y.K.; Trivedi, J.J. Capillary breakup extensional rheometry of associative and hydrolyzed polyacrylamide polymers for oil recovery applications. *J. Appl. Polym. Sci.* **2018**, *135*, 46253. [CrossRef]
11. Zhu, D.; Hou, J.; Chen, Y.; Wei, Q.; Zhao, S.; Bai, B. Evaluation of Terpolymer-Gel Systems crosslinked by polyethylenimine for conformance improvement in high-temperature reservoirs. *SPE J.* **2019**, *24*, 1726–1740. [CrossRef]
12. Hughes, A.E. The Jahn–Teller effect in molecules and crystals by R. Englman. *Acta Crystallogr. Sect. A* **1973**, *29*, 108–109. [CrossRef]
13. Cai, W.; Huang, R. Study on gelation of Partially hydrolyzed polyacrylamide with titanium(IV). *Eur. Polym. J.* **2001**, *37*, 1553–1559. [CrossRef]
14. Bai, B.; Zhou, J.; Yin, M. A comprehensive review of polyacrylamide polymer gels for conformance control. *Shiyou Kantan Yu Kaifa Pet. Explor. Dev.* **2015**, *42*, 481–487. [CrossRef]
15. Cordova, M.; Cheng, M.; Trejo, J.; Johnson, S.J.; Willhite, G.P.; Liang, J.T.; Berkland, C. Delayed HPAM gelation via transient sequestration of chromium in polyelectrolyte complex nanoparticles. *Macromolecules* **2008**, *41*, 4398–4404. [CrossRef]

16. Zhu, D.; Bai, B.; Hou, J. Polymer Gel Systems for water management in high-temperature petroleum reservoirs: A chemical review. *Energy Fuels* **2017**, *31*, 13063–13087. [CrossRef]
17. Tessarolli, F.G.C.; Gomes, A.S.; Mansur, C.R.E. Hydrogels applied for conformance-improvement treatment of oil reservoirs. In *Hydrogels*; InTech: London, UK, 2018; Available online: https://www.intechopen.com/books/hydrogels/hydrogels-applied-for-conformance-improvement-treatment-of-oil-reservoirs (accessed on 12 July 2020).
18. Li, H.; Yang, P.; Pageni, P.; Tang, C. Recent advances in metal-containing polymer hydrogels. *Macromol. Rapid Commun.* **2017**, *38*, 1700109. [CrossRef]
19. Bhatt, V. *Essentials of Coordination Chemistry: A Simplified Approach with 3D Visuals*; Elsevier Inc.: Amsterdam, The Netherlands, 2015; ISBN 9780128039373.
20. Irving, H.; Williams, R.J.P. The stability of transition-metal complexes. *J. Chem. Soc.* **1953**, 3192–3210. [CrossRef]
21. Weller, M.; Overton, T.; Rourke, J.; Armstrong, F.; Atkins, P. *Inorganic Chemistry*, 6th ed.; Oxford University Press: Oxford, UK, 2014; ISBN 0198757174.
22. Atkins, P.W. *Shriver & Atkins' Inorganic Chemistry*; Oxford University Press: Oxford, UK, 2010; ISBN 0199236178.
23. Shen, C.H.; Hsieh, B.Z.; Tseng, C.C.; Chen, T.L. Case study of CO_2-IGR and storage in a nearly depleted gas-condensate reservoir in Taiwan. *Energy Procedia* **2014**, *63*, 7740–7749. [CrossRef]
24. Lockhart, T.P.; Albonico, P.; Burrafato, G. Slow-gelling Cr3/polyacrylamide solutions for reservoir profile modification: Dependence of the gelation time on pH. *J. Appl. Polym. Sci.* **1991**, *43*, 1527–1532. [CrossRef]
25. Al-Muntasheri, G.A.; Nasr-El-Din, H.A.; Peters, J.A.; Zitha, P.L.J. Investigation of a high-temperature organic water-shutoff gel: Reaction mechanisms. *SPE J.* **2006**, *11*, 497–504. [CrossRef]
26. El Karsani, K.; Al-Muntasheri, G.A.; Sultan, A.S.; Hussein, I.A. Impact of salts on polyacrylamide hydrolysis and gelation: New insights. *J. Appl. Polym. Sci.* **2014**, *131*, 41185. [CrossRef]
27. Bruijnincx, P.C.A.; Sadler, P.J. *Advances in Inorganic Chemistry: Inorganic Reaction Mechanisms*; van Eldik, R., Hubbard, C.D., Eds.; Academic Press: Cambridge, MA, USA, 2003; ISBN 9780080915807.
28. Berger, J.; Reist, M.; Mayer, J.M.; Felt, O.; Peppas, N.A.; Gurny, R. Structure and interactions in covalently and ionically crosslinked chitosan hydrogels for biomedical applications. *Eur. J. Pharm. Biopharm.* **2004**, *57*, 19–34. [CrossRef]
29. Shannon, R.D. Revised effective ionic radii and systematic studies of interatomic distances in halides and chalcogenides. *Acta Crystallogr. Sect. A* **1976**, *32*, 751–767. [CrossRef]
30. Sydansk, R.D. A new Conformance-Improvement-Treatment Chromium(III) Gel technology. In Proceedings of the SPE Enhanced Oil Recovery Symposium, Society of Petroleum Engineers, Tulsa, Oklahoma, 16–21 April 1988; pp. 99–111.
31. Shamlooh, M.; Hamza, A.; Hussein, I.A.; Nasser, M.S.; Magzoub, M.; Salehi, S. Investigation of the rheological properties of nanosilica-reinforced Polyacrylamide/Polyethyleneimine Gels for wellbore strengthening at high reservoir temperatures. *Energy Fuels* **2019**, *33*, 6829–6836. [CrossRef]
32. Albonico, P.; Lockhart, T.P.P. Divalent ion-resistant polymer gels for high-temperature applications: Syneresis inhibiting additives. In Proceedings of the 1993 SPE International Symposium on Oilfield Chemistry, Society of Petroleum Engineers, 1993, Singapore, 8–10 February 1993; pp. 651–665. Available online: https://www.onepetro.org/conference-paper/SPE-25220-MS (accessed on 12 July 2020).
33. Lockhart, T.P.; Albonico, P. New chemistry for the placement of chromium(III)/polymer gels in high-temperature reservoirs. *SPE Prod. Facil.* **1994**, *9*, 273–279. [CrossRef]
34. Kangwansupamonkon, W.; Klaikaew, N.; Kiatkamjornwong, S. Green synthesis of titanium dioxide/acrylamide-based hydrogel composite, self degradation and environmental applications. *Eur. Polym. J.* **2018**, *107*, 118–131. [CrossRef]
35. Murugan, R.; Mohan, S.; Bigotto, A. FTIR and polarised raman spectra of acrylamide and polyacrylamide. *J. Korean Phys. Soc.* **1998**, *32*, 505.
36. Jain, R.; Mahto, V. Evaluation of polyacrylamide/clay composite as a potential drilling fluid additive in inhibitive water based drilling fluid system. *J. Pet. Sci. Eng.* **2015**, *133*, 612–621. [CrossRef]
37. Adesina, A.A.; Hussein, I.A. Impact of organoclay and maleated polyethylene on the rheology and instabilities in the extrusion of high density polyethylene. *J. Appl. Polym. Sci.* **2012**, *123*, 866–878. [CrossRef]

38. Mohamed, A.I.A.; Hussein, I.A.; Sultan, A.S.; Al-Muntasheri, G.A. Gelation of Emulsified Polyacrylamide/Polyethylenimine under high-temperature, high-salinity conditions: Rheological investigation. *Ind. Eng. Chem. Res.* **2018**, *57*, 12278–12287. [CrossRef]
39. Najafiazar, B.; Wessel-Berg, D.; Bergmo, P.E.; Simon, C.R.; Yang, J.; Torsæter, O.; Holt, T. Polymer Gels Made with functionalized organo-silica nanomaterials for conformance control. *Energies* **2019**, *12*, 3758. [CrossRef]
40. Lai, N.; Guo, X.; Zhou, N.; Xu, Q. Shear resistance properties of modified Nano-SiO_2/AA/AM copolymer oil displacement agent. *Energies* **2016**, *9*, 1037. [CrossRef]
41. Zhu, D.; Wei, L.; Wang, B.; Feng, Y. Aqueous hybrids of silica nanoparticles and hydrophobically associating hydrolyzed polyacrylamide used for eor in high-temperature and high-salinity reservoirs. *Energies* **2014**, *7*, 3858–3871. [CrossRef]
42. Masten, S. Cobalt Dust [7440-48-4] Review of Toxicological Literature. 2002. Available online: https://ntp.niehs.nih.gov/ntp/htdocs/chem_background/exsumpdf/cobaltdust_508.pdf (accessed on 12 July 2020).
43. Kim, J.H.; Gibb, H.J.; Howe, P.D. Cobalt and inorganic cobalt compounds. *IPCS Concise Int. Chem. Assess. Doc.* **2006**, 1–82.
44. Henderson, R.G.; Durando, J.; Oller, A.R.; Merkel, D.J.; Marone, P.A.; Bates, H.K. Acute oral toxicity of nickel compounds. *Regul. Toxicol. Pharmacol.* **2012**, *62*, 425–432. [CrossRef]
45. Nordberg, G.F.; Fowler, B.A.; Nordberg, M. *Handbook on the Toxicology of Metals*, 4th ed.; Elsevier Inc.: Amsterdam, The Netherlands, 2014; Volume 1, ISBN 9780123973399.
46. Shaker, A.M.; El-Shahawy, A.; Zaki, A.H.; Abdel-Rahim, E.F.; Khedr, M.H. Estimation The median lethal dose and inhibitory concentration of Tio_2, Sio_2, Zno and Cuo nanoparticles on human hepatoma HEPG2 Cells. *Int. J. Pharm. Phytopharm. Res.* **2017**, *7*, 18–23.